NDE2002 predict. assure. improve.
National Seminar of ISNT
Chennai, 5. – 7. 12. 2002
www.nde2002.org

X-Ray Imaging Systems for NDT and General Applications

M. Kröning[1], O. Hirsch[1], B. Shulgin[2], D. Raikov[2], M. Kidibaev[3], T. Koroleva[4], R. Hanke[5], T. Baumbach[1]

[1]Fraunhofer Institute for Nondestructive Testing, Saarbrücken and Dresden, Germany
[2]Urals State Technical University, Ekaterinburg, Russia
[3]Issyk-Kul State University, Karakol, Kyrghys Republic
[4]National Academy of Sciences, Bishkek, Kyrghys Republic
[5]Fraunhofer Institute for Integrated Circuits, Applied Electronics Department, Erlangen, Germany

1. Introduction

For more than 100 years, conventional X-ray radiography has been applied in medicine and nondestructive testing (NDT) for the investigation of the spatial distribution of matter in objects and organisms; X-ray techniques work nondestructively.

Depending on material density, geometry, and applied energy, X-rays are able to penetrate solid materials from the nanometer-range down to a depth of several centimeters. Because of this relatively high penetration depth, buried or hidden structures, boundary layers, and defects can be imaged and evaluated. Images taken by digital X-ray sensors are immediately available in electronic form and can be digitally transmitted, stored, and evaluated at remote locations. X-ray sensors are therefore a precondition for an intelligent image evaluation such as the application of digital, real-time detectors for X-ray tomography.

Currently, micro-tomography and high-resolution radioscopy typically allow for a local resolution of 100 – 10 µm. Hereby, the pixel size of commercial array detectors is limited to 400 - 100 µm, and the focal spot of micro-focus tubes is about 5 microns, depending on their type. The high local resolution of these systems can only be achieved through the geometrical object enlargement by placing the object close to the X-ray focal spot in the beam cone. Low-noise local resolution down to sub-micrometer range needs further development of:

- Improved X-ray sources, such as high-performance targets or synchrotron radiation sources.
- Realization of new detector concepts and their optimization for NDT systems.

Since recently, it was possible to limit the active focal spot to less than 1 µm for high-resolution imaging. However, the small spot size, the usually large distance between object and detector, and typical exposure times between 100 ms and 1 s, limit the radiation output for low-noise images.

Whereas sensor arrays for the visible spectrum have already reached a high development stage, imaging sensors for X-rays and infrared spectral range are just at the beginning of their development. X-ray array sensors will replace conventional X-ray film technique in medical, dental, NDT applications and at security and customs screening stations. Innovative digital detector technologies are fundamental for tele-medical applications and telematics for industrial process monitoring and security applications. They integrate features to forward individual sensor signals or pre-processed images to specialists via the internet for further processing and evaluation.

2. Imaging X-ray Detectors - A Short Review

X-ray detectors are offered and applied on the basis of a variety of different physical principles and technical implementations. Figure 1 shows an overview.

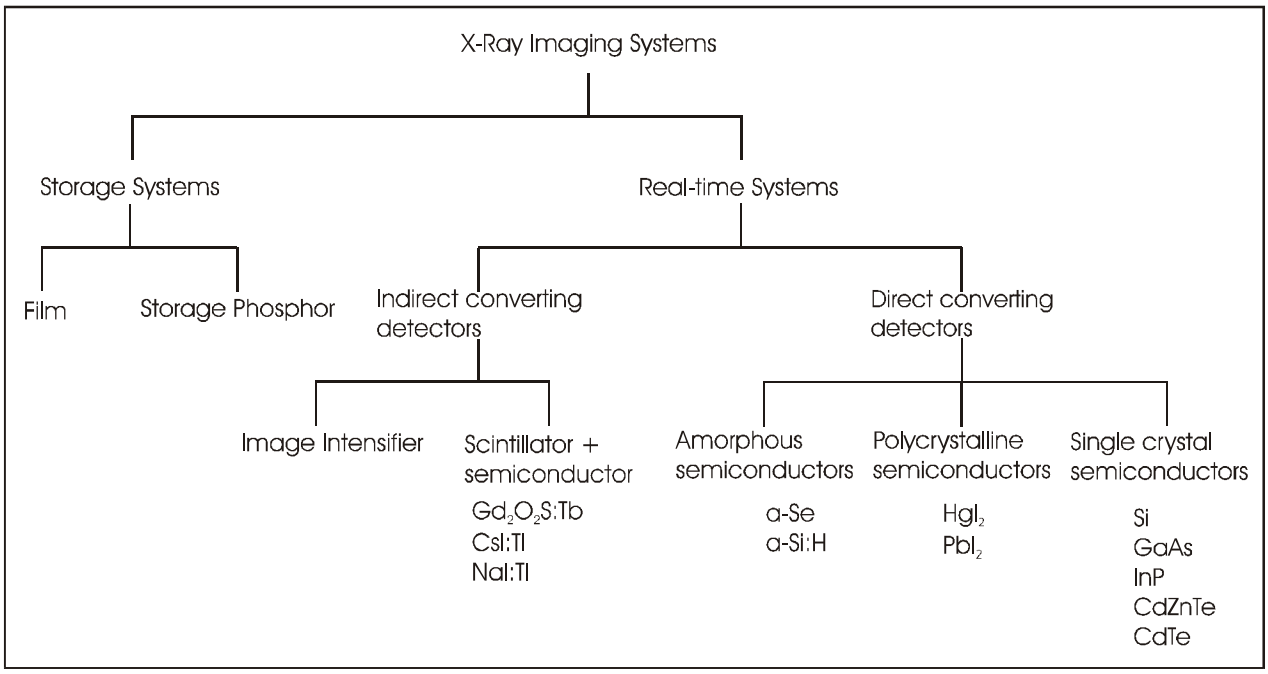

Figure 1: Overview of X-ray imaging systems

There are memory systems and real-time systems. The classical storage medium is the X-ray film, which still offers the highest local resolution. Frequently, due to higher computer compatibility, radiographic films are subsequently digitized [1]. However, the chemical development process, non-reusability, and noise contribution by the granulation of the film adversely affects the range of applications.
Storage phosphor screens ("image plates") reduce the exposure time by about 50% to 90% compared to X-ray film systems. In the crystals of these storage media, electrons are trapped on deep levels after interaction with imaging X-rays. Thus, image information is stored in form of a latent picture. The trapped electrons can be stimulated by irradiation with visible laser light. The laser light results in a photo-stimulated fluorescence light, which is used for final image generation. An example of a storage phosphorus is $BaFBr:Eu^{3+}$. The irradiation by He-Ne laser (λ = 633 nm) produces fluorescence light with λ = 390 nm. The information stored on the image plate can be erased by illumination with white light.
Real-time detectors are needed for in-situ investigations and X-ray tomography. These detectors generate the information from the image directly in computer-readable form. Basically, there are two groups of real-time detectors: 1) *indirect converting sensors,* converting X-rays into visible light; and 2) *direct converting sensors* with direct release of electrical charges caused by the absorbed X-ray quanta.
Well-known indirect converting systems are image intensifiers. The systems are composed of a vacuum tube with a photo-cathode on one side and a luminescent

screen on the opposite side. Amid both screens, the electron beam system scans the photo-cathode and generates the image on the luminescent screen. The visible luminescence light is registered [2].
Today *scintillating detectors* are more important. Scintillating screens convert the incoming X-rays into visible light. The classical set-up for scintillating systems consists of NaI:Tl with a photo-multiplier. In modern systems, scintillating screen and read-out electronics are assembled into a compact unit. Actual development trends are described in [3]. Nowadays, efforts are made on exploring more effective scintillating materials (see chapter 5). In principle, the dual radiation conversion is unfavorable reducing the sensor efficiency.
Direct converting X-ray sensors represent the newest, most promising development line. The sensor principle is based on direct interaction of X-rays with the semiconductor material and generating Electron-hole pairs. In the applied electrical field, the electrical charges move to the edges of the semiconductor where they are read by microelectronic circuits. Amorphous, polycrystalline and single-crystal semiconductors are used today (chapter 5).
At present, the development of direct and indirect converting semiconductor detectors is rapid and most promising.

3. Requirements for digital X-ray detectors

Due to the variety of applications for digital X-ray detectors, different specifications have to be considered. X-ray sensor cannot be optimized for all application areas simultaneously. First of all, the sensor must be sensitive in the applied energy range for the specific measurement problem. Commonly used X-ray energies may range from keV to meV. Highly efficient sensors can only be achieved under the following conditions:

1. The detector layer must absorb the imaging radiation almost completely.
2. Each X-ray quantum must produce as many charge carriers as possible in the detector.
3. The loss of charge carriers (in semiconductor pairs of electrons and holes) by re-combinations, etc., must be minimized.

Therefore, material research for X-ray sensors has become essential to meet these requirements and to optimize material properties and thicknesses of the sensitive detector layer as a function of the X-ray spectrum (see chapter 5).
Furthermore, the *signal-to-noise ratio* (SNR) of the image produced by the detector must be considered as a crucial criterion. The *Detective Quantity Efficiency* (DQE) can be used for SNR optimization [4]. It is defined as:

$$DQE(\upsilon) = \frac{(S/N)^2_{out}(\upsilon)}{(S/N)^2_{in}(\upsilon)}$$

S: signal amplitude; N: noise power spectrum; ν: spatial frequency;

Certainly, detector efficiency is a prerequisite for a good SNR. A photon of energy E_γ produces a charge Q_0 in the detector:

$$Q_0 = q \cdot \frac{E_\gamma}{E_{e/h}}$$

$E_{e/h}$ represents the material dependent energy for the production of an individual electron-hole pair (Table 1), and q is the elementary charge.

The Charge Collection Efficiency (CCE) indicates Q, which is the actually provable charge at the electrodes in relation to Q_0:

$$CCE = \frac{Q}{Q_0} \cdot 100\% \quad .$$

At low energies, modern semiconductor detectors possess a CCE of > 99%. The CCE decreases with rising photon energy (see chapter 5).

In respect to the *detector area*, large detectors are distinguished with active surfaces areas of up to (60 x 60) cm^2, which are partly suitable for the direct refurbishment of radiographic film devices by digital radiography, and small high-resolution detectors with active surface areas of several square centimeters. FlashScan 30 of dPix LLC (USA) with a surface of 30 x 40 cm^2 exemplify a large-sized detector [5]. The attainable resolution is determined by the pixel size. For large area detectors, it ranges between 120 to 400 µm. Today, high-resolution X-ray detectors with pixel sizes of approximately 20µm are already available [6].

The optical characteristics of image detectors are closely related to the pixel size. Contrast Transfer Function (CTF), Modulation Transfer Function (MTF), and Line Spread Function (LSF) are used for the characterization in consideration of the detector and the optical transfer system.

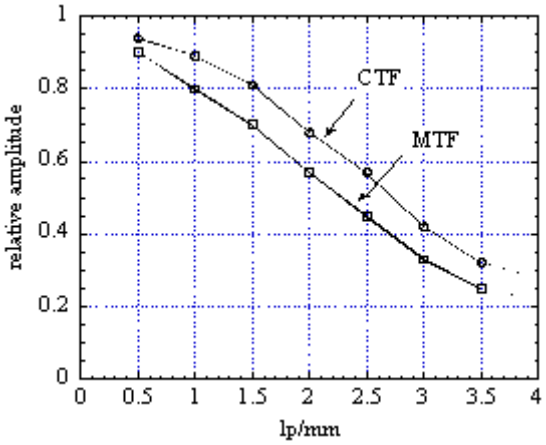

Figure 2: Contrast transfer function (CTF) and modulation transfer function (MTF) for an imager with pixel size of 127 µm [7]

The contrast (C) of an image is defined through the maximum range of radiation intensity normalized to the maximum intensity I_{max}:

$$C = \frac{I_{\max} - I_{\min}}{I_{\max}} \quad .$$

The Contrast Transfer Function (CTF) indicates the relation of the contrast for a spatial frequency (ν) to the contrast for ν=0, with a bar pattern as the input for the optical system. The CTF decreases with an increasing spatial frequency, and specifies the maximum resolution of line-pairs/mm (lp/mm). The Contrast Transfer Function for sinusoidal intensity samples is given by the Modulation Transfer Function MTF. This function indicates the relation of the output modulation intensity versus the input intensity modulation. Thus, the transfer system is characterized by the Line-Spread Function (LSF), and represents the pulse response function of an optical system and indicates the widening of an infinitely small line by the system.

Details for the determination of the mentioned functions are given in [8]. Figure 2 shows CTF and MTF for a detector with a 127 µm pixel size.
The maximum *read-out rate* depends on the number of pixels, the applied technique, and the organization of the read-out circuit (serial/parallel). Particularly for X-ray tomography and real-time radiography, very high read-out rates are necessary. At present, read-out times of 250 µs for a 64 kpixel matrix have already been accomplished [9].

4. Indirect and Direct Converting Semiconductor Detectors

The structure of an indirect converting X-ray sensor with scintillating screen is shown in Figure 3. For the assembly of the photodiode matrix, different versions are available (see chapter 6). For a good overall efficiency, the emission characteristic of the scintillator must be adjusted to the spectral response-curve of the photodiodes. Figure 4 shows examples for the emission characteristics of scintillating screens. In contrast to X-ray films, the detector response to exposure is linear – a great advantage, but has a limited image definition due to the isotropic emission of fluorescence light.

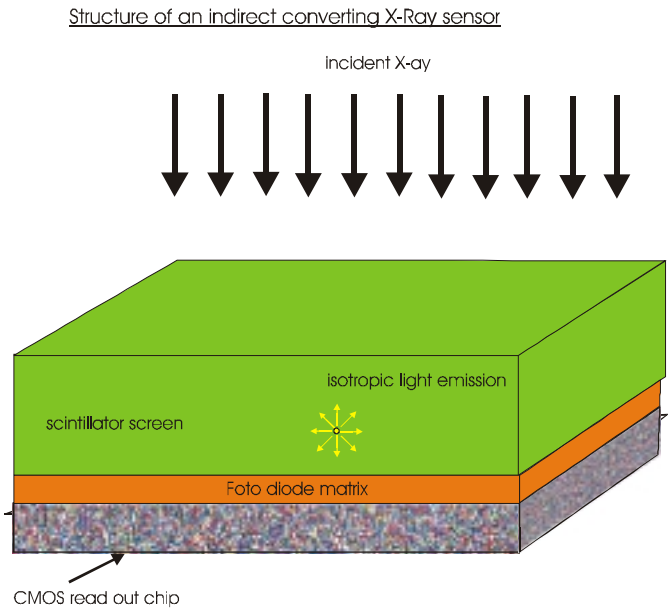

Figure 3: Schematic assembly of an indirect converting X-ray detector

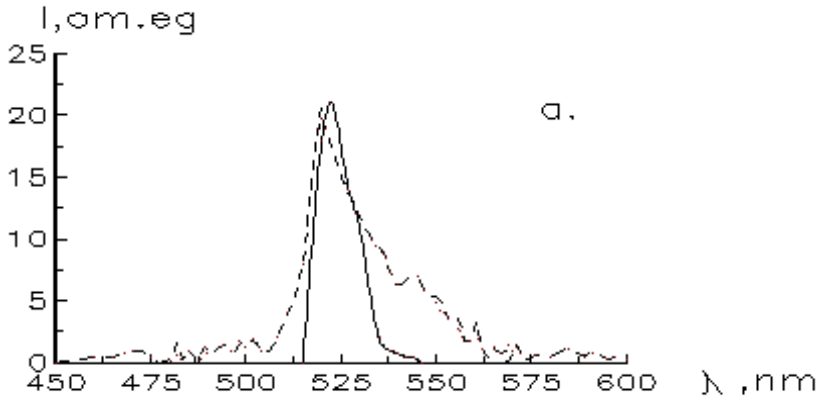

Figure 4: Spectra of radio-luminescence of crystals: a) LiF: U; Fe (0,1 mol. %) and

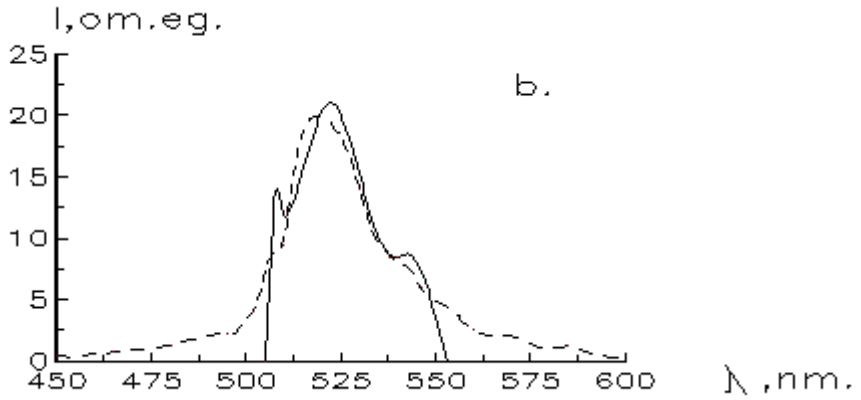

Figure 4: Spectra of radio-luminescence of crystals:
b) LiF: U; Fe (0,01 mol. %), registered in current (continuous line) and pulse (dotted line) modes

Figure 5 shows the typical assembly of a direct converting semiconductor X-ray detector. For technical details of the structure see Chapter 6. The incoming X-ray photons interact with the detector material predominantly through three effects: 1) photo effect, 2) Rayleigh (or elastic) scattering, and 3) Compton (or inelastic) scattering. At energies of up to 100 keV, the photo effect is dominating [8]. One photo-electron generates about 10000 electron-hole pairs.

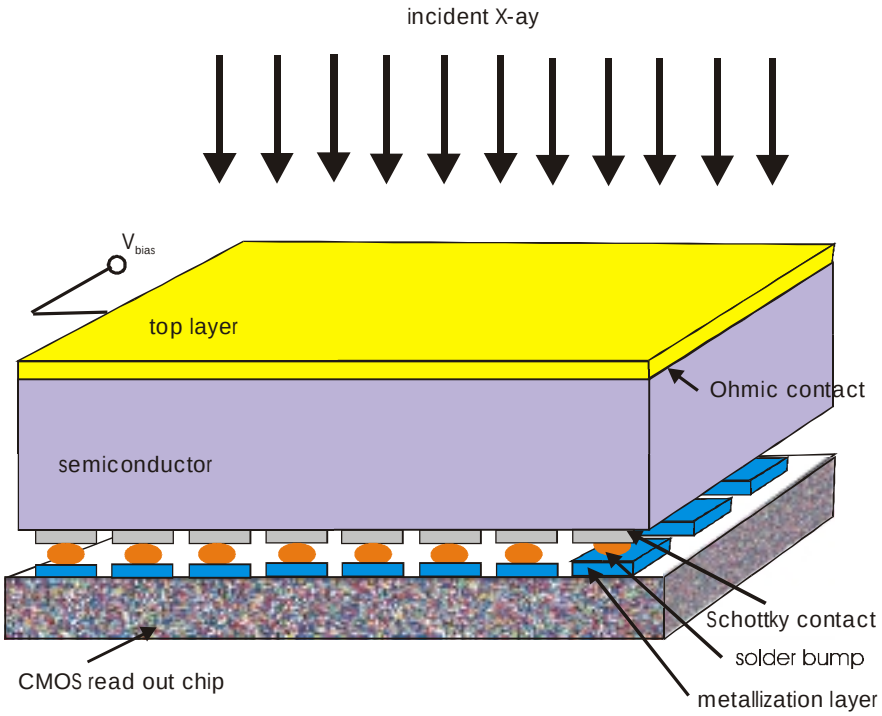

Figure 5: Schematic assembly of a direct converting X-ray detector with bump bond connections to the read-out circuit

Both, electrons and holes are charge carriers. Electrons and holes are separated by the applied electric field, and they move in opposite directions from the electrodes. The strength of the electrical field is approximately 106 V/m. This high field strength

is required to sensitize the entire detector volume to the applied radiation. The input circuitry of the read-out electronics (charge sensitive amplifier) is connected to the bottom electrode.
The presented design corresponds to a matrix of Schottky diodes. Other designs are used likewise, among them are P-I-N detectors (a sequence of semiconductors of p-, i- and n-type) [10], and M-I-S detectors (metal, i-type semiconductor, p- or n-type semiconductors) [11]. Compared with Schottky diode detectors these devices are characterized by a more homogeneous electrical field and (mostly) a higher breakdown voltage.
The thickness of the detector layer is a parameter for optimization; the thicker the layer, the better the absorption (see Figure 6). However, due to trapping effects, the probability of charge losses is higher with the increase of the layer thickness.

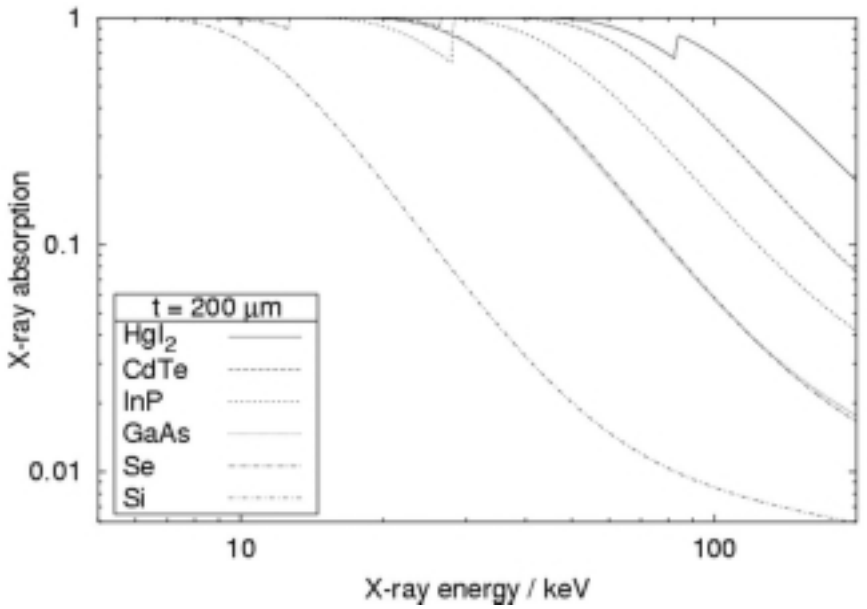

Figure 6: Absorption efficiency of various detector materials vs. energy for a detector layer thickness of t = 200 µm

5. Materials

The appropriate selection and the quality of the sensor materials determine the quality of radiation sensors substantially. For this reason, much attention is dedicated to the development of sensor materials.

5.1 Scintillator systems

In general, the requirements for scintillation materials are:

- High X-ray absorption
- High light output with good spectral matching to the PIN photodiode (400-800 nm)
- Fast decay (τ < 0.1 ms) for the main components of light emission

Some single crystal scintillators meeting these specifications are presented in Table 2, and are compared to standard NaI-Tl detectors. New compounds are currently

investigated intensively. Here, we present results of the Urals State Technical University.
At the Urals State Technical University, a La_2O_2S-Ce scintillator was proposed [12] analogous to the Gd_2O_2S-RE scintillator, developed by Siemens AG [13] simultaneously. Some compounds have been investigated in collaboration with the Institute of Physics NAS of KR and Issyk-Kul State University [14-16,23-25]. More than 160 inventions have resulted in:

- Inorganic scintillators based on $LiF\text{-}UO_2(NO_3)_2$ [14]
- Inorganic scintillators based on $LiF\text{-}UO_2(NO_3)_2\text{-}CuF_2$ [15]
- Storage luminophor based on LiF-U,Ti [16]
- Scintillation wave-guide detectors based on AgCl-AgBr [23]

Scintillation wave-guides, based on mixed silver halides [22, 23], are considered for future generation of two-dimensional detector systems (see Table 3).
Some effective red and IR-scintillation materials with good spectral matching to the photodiode were subject of investigations: InP (λ=855 nm), GaAs (λ=790-890 nm), $MgAl_2O_4$ (λ=675-725 nm), $Bi_2Ga_4O_9$ (λ=610-710 nm), HgI_2 (λ=530-650 nm).
The HgI_2 compound is known to be both, a semiconductor and luminescence detector [17-20]. Under X-ray excitation (300 KeV) the luminescence spectrum of HgI_2 shows 3 bands: 534, 584 and 630nm [17]. The 584nm band (decay time <100 ps) is related to an edge luminescence of non-relaxed excitons. Its structure is determined by exciton-phonon interaction. The 534nm band results from super edge luminescence (it was found earlier for laser excitation [26]). The 630nm band (decay time 1.1 μs (30%) and >10 μs (70%)) is caused by defects (impurities).
The cooling of HgI_2 specimens leads to an increase of the signal output of (536 nm) edge- and (608 and 630 nm) impurity luminescence. The luminescence spectrum of the super fast component scintillation (<100 ps) is probably due to capture of excitons on lattice defects.
The discovery of this super short (fast) component (<100 ps) scintillation of red HgI_2 helps to increase the loading ability of electronic tracts and thus for faster registration of X-ray signals.
The calculated light collection coefficients ($K_{L,C}$) for HgI_2 crystals with mirror and rough surfaces for different thicknesses are:

Thickness, mm	KL,C (mirror surface)	KL,C (rough surface)
2	0.096	0.331
4	0.091	0.237
6	-	0.140

HgI_2 crystals with a thickness of 2 to 4 mm will register 100 keV X-rays with an efficiency of 0.974 and γ-radiation at 1 to 5 MeV with an efficiency of 0.12-0.39 [17].

5.2 Direct converting systems

Highly integrated read-out electronics of modern sensors are manufactured in silicon CMOS technology. When silicon is used as detector layer, the entire element can be manufactured on a single substrate [27]. Unfortunately, the use of silicon is limited to low X-ray energies E < 20 keV because of its low absorption. For higher energies a

variety of other materials is under investigation. Table 1 shows materials presently being evaluated for usability.

Amorphous Semiconductors can be relatively simply manufactured for a large application range. Therefore, they are important for flat panel detectors. In the meantime, Hologic Inc., in the USA [28], is producing large area detectors that are based on amorphous selenium. Unfavorable features are the high energy of 50eV needed for the production of one electron-hole pair and the high probability of re-crystallization when exceeding an upper temperature limit.

Today, *Single Crystal Semiconductors* are available for both, wafer and epitactic grown material. A typical representative is germanium, which possesses an excellent energy resolution; however, it must be used at low temperatures because of its small band width of 0.72 eV.

Silicon is used as single-crystal and polycrystalline detector material.

Presently, GaAs is frequently used as detector material [29]. For this material, well developed technologies are applicable. For detectors, carbon or chromium composite semi-insulating GaAs is used. GaAs is a composite material with high charge carrier mobility. Charge-trapping by the EL2 defect and the short charge carrier lifetime presents difficulties. The absorption of X-ray quanta is much better than in silicon (see Figures 6 and 7).

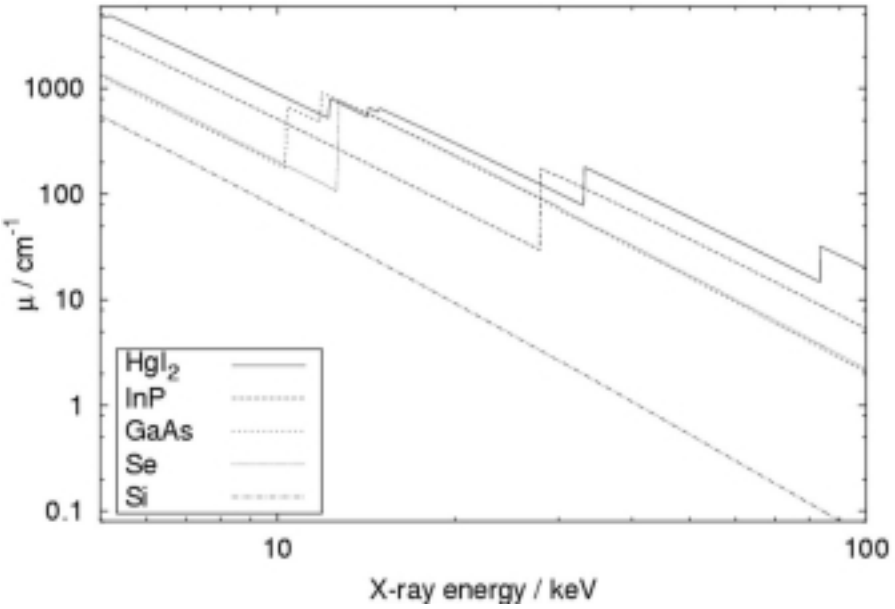

Figure 7: Energy dependent linear attenuation coefficient μ of various detector materials

In the future, Indium Phosphate could gain some importance as a detector material [30]. At present, InP detectors must still be operated at low temperatures. Similar as in GaAs, the electrons in InP are very mobile.

CdTe and CdZnTe possess good characteristics for spectroscopic and imaging applications. These materials require a very careful handling, since they are relatively brittle.

Besides Polycrystalline Silicon, some Polycrystalline materials from heavy elements become generally accepted. Here, PbI2 and HgI2 are to be mentioned. With medium nuclear charge numbers of higher than 62, they possess an extraordinary good absorptive capacity (see Figures 6 and 7). Different coating technologies were developed to allow an economic production of large area detectors [31].

6. Detector Electronics

Radiation effects produce electrical charges in all semiconductor X-ray detectors. For detection, the associated increase of conductivity of a semi-insolating semiconductor is used, or the produced charges are registered. The read-out electronics can be designed for the integrating mode or the counting mode.
In the first case the electrical charges are accumulated during the exposure time in a simple condenser or in an integration amplifier; the electronic circuit is designed accordingly. After exposure, an analog digital converter (ADC) digitizes the signals. Since separate ADC's for each pixel are not reasonable, a multiplexer successively switches the individual pixels to the ADC. A substantial disadvantage of this procedure consists of integrating dark currents of the detector elements. Therefore, a special dark current compensation is necessary.
The counting version of read-out electronics is characterized by single photon registration. Here, it is necessary to implement an own counter for each pixel, which can be realized in a highly integrated CMOS technique only. Using a comparator, a threshold level for the signal amplitude is adjusted in such a way that it is placed significantly above the noise level of the detector. Each photon produces a signal peak value above the threshold value. This way, a particularly favorable signal to noise ratio can be obtained. Since different photon energies generate differently high signal amplitudes, an energy-selective detection can be performed. Herewith, a new quality of radiation detection is achieved, which principally enables spectroscopic imaging. The technical efforts for counting mode detectors are extremely high. Nevertheless, circuits base on this principle have been developed with up to 64k pixels and down to 55 µm pixel size [9].
The counting method is not applicable for materials with low mobility charge carriers and very large detector thickness, since the electrical pulses are stretched and single pulses mutually overlap themselves due to the charge carriers drifting time.

7. Design

In the meantime, some imaging X-ray detectors designs have become generally accepted. Large and Small Area detectors and High-Resolution detectors are always different in design.
Large Area Detectors are mostly designed as so-called flat panel detectors. Their mechanical basis consists of a glass substrate. Above this, read-out electronics are installed in thick film or thin film technique (Thin Film Transistor, TFT). The electronics consists of relatively simply structured matrix of electronic switches. The produced electrical charges are collected in an integrated capacitor during the exposure, and are afterwards transported to charge-sensitive amplifiers and analog/digital converters at the edge of the matrix.
For a direct converting sensor, a detector layer, based on an amorphous or polycrystalline semiconductor, is placed on this matrix. Typical examples of this design are the already mentioned FlashScan 30 of dPix LLC, USA (amorphous silicon) and the DirectRay detector of Hologic Inc., USA (amorphous selenium, 35 cm x 43 cm). Direct converting flat panel detectors based on HgI_2 polycrystalline from Real-Time Radiography Ltd, Israel represent a new development, and are superior to conventional detectors in the upper energy range.
For indirect converting sensors, a matrix of photodiodes is additionally placed on the glass substrate (Thin Film Diode, TFD). On the top side is the scintillation layer, e.g.

CsI:Tl or Na:Tl. PIXIUM 4600 by Trixell Company, France (43 cm x 43 cm, 9 millions pixel, 143 µm pixel size) exemplifies such a type of a modern device.
Flat panel detectors with read-out electronics in CMOS technology are also available. For example, Hamamatsu Corp., USA, offers the type C 7942, which is based on a CsI scintillator with an active surface of 12 cm by 12 cm and 50 µm pixel size.
Read-out chips in silicon CMOS technology establish the base for *high-resolution sensors*. In comparison with TFT-matrices, CMOS read-out chips feature a variety of advantages. CMOS (Complementary Metal-Oxide-Semiconductor) represent a technology, in which circuits are based on transistors of two conductivity types (n-channel and p-channel). CMOS circuits consume very little energy. Because of the low power dissipation, the integration density is very high. In 0.25 µm CMOS technology, a 1 mm^2 chip area can hold more than 100,000 transistors. This helps to design very complex circuits directly on the sensor chip. The sensor integrates a pre-amplifier for each individual pixel, dark current compensation, a threshold switch, and a counter (for photon counting sensors). Thus, signal pre-processing can be performed inside the sensor and photon counting sensors are possible.
In a monolithic sensor, the substrate of the chip is used as a radiation-sensitive layer. The charges of the pixels can be transported, e.g., using an analog shift-register to the charge-sensitive amplifiers, which results in a Charge Coupled Device (CCD). So far, these types of devices could only be manufactured on silicon wafers, which possess the well-known disadvantages concerning absorption. Up to now, only one implementation in GaAs technology is known [32]. Other detector materials require a hybrid solution with silicon CMOS read-out on detectors of another material. A possible technology is known as TFA (Thin Film on ASIC) (see [33] and Figure 8). This technology is suitable for sensors for which the radiation-sensitive layer is amorphous or polycrystalline. ASIC is the abbreviation for “Application Specific Integrated Circuit”.

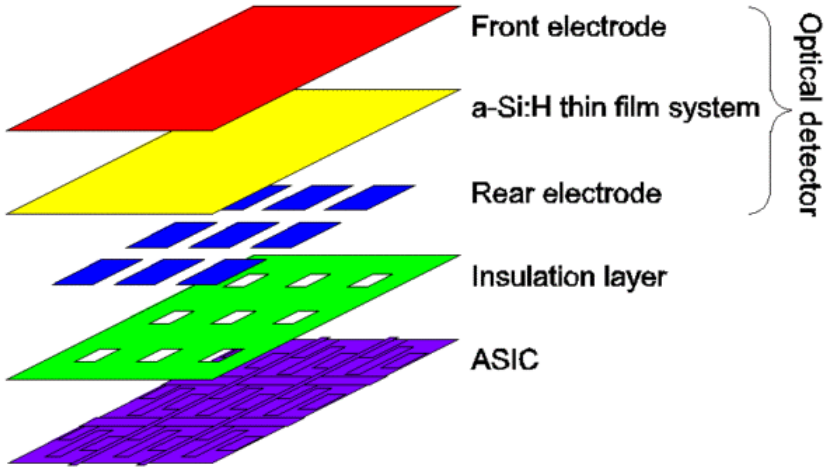

Figure 8: Layer sequence of TFA technology (University of Siegen)

For the mechanical and electrical connection of single crystalline detector layers with CMOS electronics, the bump-bonding technology is favored (see Figure 5). Both components are connected by a multitude of tiny soldering balls. For each pixel a separate contact is necessary. Both, the upper side of the CMOS chip and the lower surface of the detector layer are divided into pixels with an optimized metallization.

The limited chip size of CMOS read-out chips of about some square centimeters are a disadvantage of this technology. Expansion to larger surfaces requires the use of several joined chips.
For NDT applications, CMOS sensors are sometimes too small. Therefore, arrangements of several single sensors on a ceramic substrate are under development. For

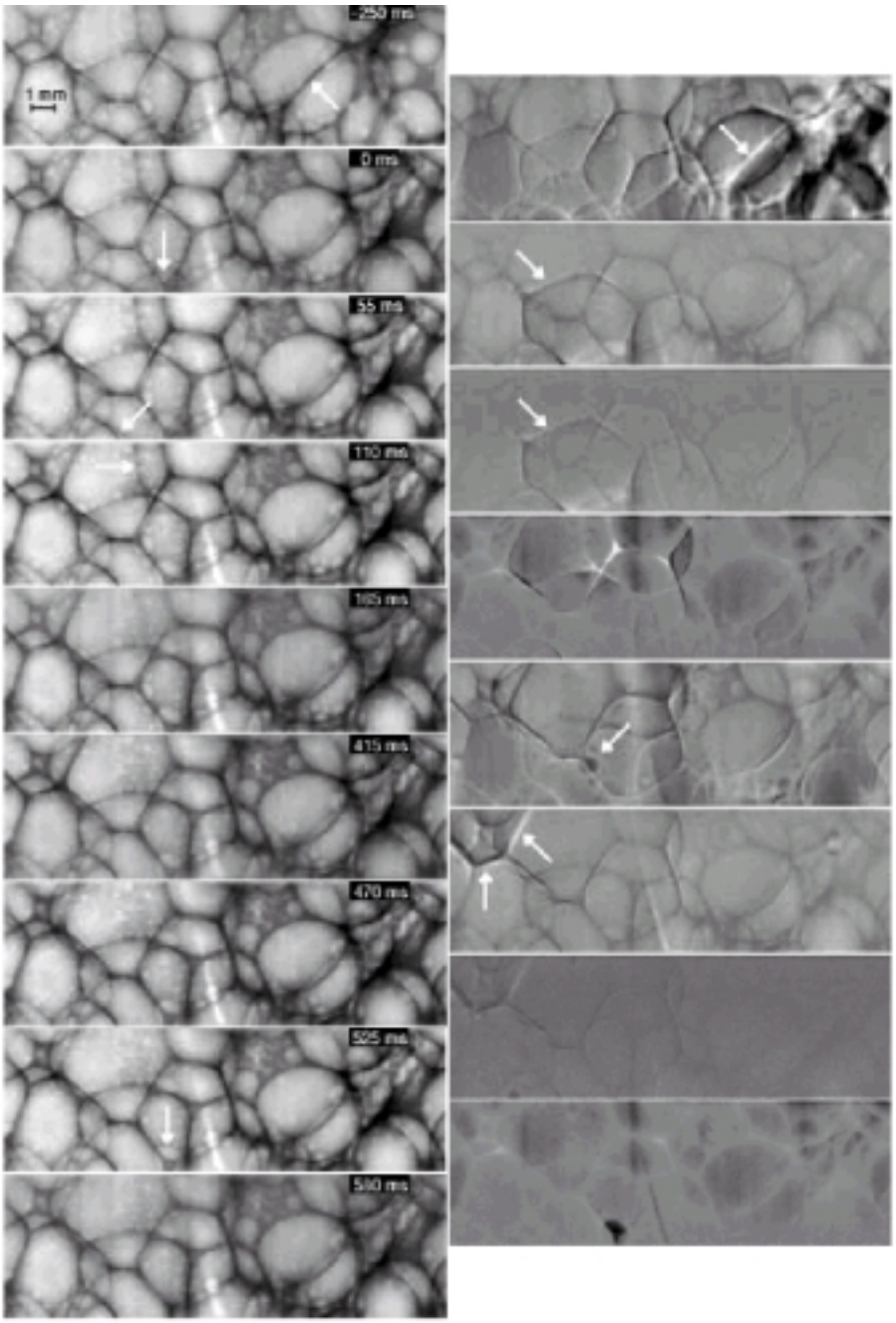

Figure 9: Fast radiography visualizes in-situ the collapse of a liquid metal foam which has been foamed in a furnace at a temperature of 775 °C. The difference images between two successive frames show the rearrangement of the liquid metal: white indicates vanishing, black appearing metal. Pixel size is 30 μm.

example, an array of 8 single sensors was presented by Medipix collaboration (CERN). Large flat panel detectors can favorably replace X-ray films, but they are still very expensive. If the exposure time is not crucial, line sensors can be used instead.

Today, computers are a standard component of image recording systems. The data transfer between detector and computer is managed using special I/O cards. In the future, sensors and computer can be connected through fast standard interfaces (e.g. “Fire Wire” IEEE 1394).

8. Prospects – Usage of X-ray Sensors in NDT Systems

Real-time digital image processing based on digital sensor arrays opens completely new application areas for X-ray inspections. Exciting developments are underway, and new dimensions of X-ray imaging are already apparent [34-37].
New X-ray systems provide information on material structures and processes, for which it was just a dream only 10 years ago. As example, solid metal foams can be employed for light-weight construction with good energy dissipation requirements and are thus interesting for ground transportation vehicles and aerospace applications. Fast radiography is a very helpful technique for visualizing the decay of metal foams in the liquid state which allows to draw conclusions on the physics of foaming [34] and foaming technology [37]. Fig. 9 shows an example for an in-situ investigation of the foaming process of an Al alloy foam. A careful analysis of future NDT systems is imperative to keep the competitiveness in broad areas of industrial NDT and consumer applications.

Table 1: Materials for direct converting X-ray detectors

Material	Atomic number	Average atomic number	Density (g/cm^3)	Bandgap (eV)	Energy per e/h pair (eV)	Drift mobility electron (cm^2/Vs)	Drift mobility hole (cm^2/Vs)	Free drift time electron (s)	Free drift time hole (s)	γ-Ray energy resolution @ 60 keV FWHM (keV)	Remarks
diamond	6	6	3,52	5,47							
Si	12	12	2.33	1.12	3.6	1450	450	$>10^{-4}$		0.4	
Ge	32	32	5.33	0.72	2.98	36000	42000	$>10^{-4}$		0.3	@ T=77K
GaAs bulk	31/33	32	5.32	1.42	4.3	>8000	400	10^{-9}-10^{-8}		8.0	
GaAs epi.									$4 \cdot 10^{-5}$	2.5	
AlSb	13/51	32	4.26	1.62	5.05						
InP	49/15	32	4.79	1.35	4.2	4600	150				
GaSe	31/34	32.5	4.55	2.03	6.3[1], 4.5[8]	60	215				
a-Se	34	34	4.3	2.2[6],1.7-1.9[7]	50[6]						
CdSe	48/34	41	5.74	1.75		720	75			8.5	
Bi_2S_3	83/16	42.8	6.73	1.3							
$Cd_{0.8}Zn_{0.2}Te$	48/30/52	48.2	6	1.6	5.0	1350	120	10^{-6}	$2 \cdot 10^{-7}$	2.5	
CdTe	48/52	50	6.06	1.52	4.43[1]	1000	80	10^{-6}	10^{-6}	1.7	
Poly-TiBr	81-35	58		2.7	2.7						
HgJ_2	80-53	62	6.30	2.1	5.5[6]	100	4	$7 \cdot 10^{-6}$	$3 \cdot 10^{-6}$	0.9-1.8	
PbI_2	82/53	62.7	6.16	2.6 ,2.3[6]	7.68[1], 6.6[6]	8	2	10^{-6}	$3 \cdot 10^{-7}$	1.83	

Sources for Table 1:

1) Jürgen Giersch, Physikalisches Institut, Universität Erlangen- Nürnberg, Kolloqiumsbeitrag, 05/04/2001
2) M. Schieber et al., Nondestructive Imaging with Mercuric Iodide Thick Film X-ray Detectors, Advanced NDE Symposium, Newport Beach 3/4/2001
3) http://www.simage.fi/technology/
4) Fax „Siemens Festkörper-Matrixdetektoren“ May 1997
5) http://www.directradiography.com/press/releases/1999/agfa-pr-us.htm P.-K. Soltani, D. Soltani, D. Wyshewski et al., Amorphos Selenium Direct Radiography for industrial Imaging, DGZFP-Proceedings BB 67-CD, Berlin, March 15-17, 1999
6) G. Zentai et al., Large area mercuric iodide thick film X-ray detectors for fluoroscopic (on-line) imaging, SPIE-MI 4682-62
7) J.-P. Moy, Recent developments in X-ray imaging detectors, Nucl. Instr. and Meth. A 442 (2000) 26-73
8) D. S. McGregor, H. Hermon, Room-temperature compound semiconductor radiation detectors, Nucl. Instr. and Meth. A 395 (1997) 101-124.

Table 2: Properties of Scintillators

N	Scintillator	B, %	R, %	τ, ns	λ, nm
1.	NaI-Tl	100	7	230	415
2.	LiF-Cu,Ti,U	2-6	-	10	460, 520
3.	NaF-Cu,Ti,U	2-5	-	10-14	474, 500, 520
4.	SrF_2-Tb	10	40	100, 4200	380, 546
5.	Y_2SiO_5-Ce,Tb	160	10-12	60	420, 546
6.	Gd_2SiO_5-Dy	14	15	15	480, 580
7.	La_2O_2S-Ce	10	-	10, 1200	450-500
8.	Lu_2SiO_5-Ce	70	10-12	20	420
9.	Na_2ZrSiO_5-Eu,Tb	15-20	25	50-70, 420	320, 546
10.	$Gd_3Sc_2Al_3O_{12}$-Ce	8	70	40, 1500	570
11.	$Bi_4Ge_3O_{12}$	10	17	60, 300	495
12.	$Pb(Mo,W)O_4$	7	70	5-10	475

B: light output; R: resolution; τ: decay time; λ: wavelength

Source: B. Shulgin, Fast inorganic scintillators, Proceedings of LUMDETR'91, Riga, Latvia, 1991, p.A3

Table 3: Properties of scintillation materials

	Materials	Density, g/sm^3	Wavelength, nm	Decay time γ- scintillation, ns	Index coefficient	Output, %	Hygroscopicity	Temperature span, °C	Possibility to pull the crystal
1.	NaI-Tl	3,67	415	230	1,85	100	yes	-30…+150	no
2.	CsI-Tl	4,71	550	450/~1 μs	1,79	30–45	yes	-30…+150	1-2 mm
3.	CaF_2-Eu	3,18	435	940	1,47	50	no	-30…+150	no
4.	$Bi_4Ge_3O_{12}$	7,13	480	300	2,15	15–20	rela-tive	-30…+150	no
5.	Y_2SiO_5-Ce	4,45	420	20	1,8	45	no	-30…+150	no
6.	Lu_2SiO_5-Ce	7,4	420	20–40	1,82	375	no	-30…+150	no
7.	^{6}Li-glass	2,6	390–430	60	1,56	4–6	no		no
8.	ZnSe-Mn	5,42	585	1–10	2,6	4–6	no	-60…+200	no
9.	ZnSe-Mn,Cu,Al	5,42	630	1 μs	2,6	6–8	no	-60…+200	no
10.	$CdWO_4$	7,90	470-540	20/30 μs	1,94	17–92	no	-10…+100	no
11.	Plastic	1,03	375–600	2–8	1,58	30	no	0…+30	yes
12.	CsI-Na	4,51	420	630	1,84	85	yes	-30…+150	1-2 mm
13.	BaF_2	4,88	310	630	1,5	16	relati-ve	-5…+200	no
14.	Gd_2Si0_5-Ce	6,71	440	30–60	1,85	20–25	no	-5…+200	no
15.	LiI-Eu	4,08	470	1400	1,96	35	yes	-5…+200	no
16.	ZnSe-Te	5,42	610-640	3/~50	2,6	20,84	no	-60…+200	no
17.	Fiber scintillation light guide	6,4	400-510		2,1-2,2	80	no	-60…+200	50 m and more

References

[1] U. Zscherpel, Film digitisation systems for DIR: Standards, Requirements, Archiving and Printing, Jour. of Non-Destructive Evaluation, 20 (2000) 53-56

[2] M. Rossi, F. Casali, S. V. Golovkin, V. N. Govorun, Digital radiography using an EBCCD-based imaging device, Appl. Radiation and Isotopes 53 (2000) 699-709

[3] E. Hell, W. Knüpfer, D. Mattern, The evolution of scintillating medical detectors, Nucl. Instr. and Meth. A 454 (2000) 40-48

[4] K. Stierstorfer, M. Spahn, Self-normalizing method to measure the detective quantum efficiency of a wide range of x-ray detectors, Med. phys. 26 (1999) 1312-1319

[5] http://www.dpix.com/products.html

[6] http://www.esrf.fr/experiments/ISG/SpecialDetectors/AreaDiffraction.php#SAXS

[7] J. M. Casagrande, A. Koch, B. Munier, P. de Groot, High Resolution Digital Flat-Panel X-Ray Detector- Performance and NDT Applications, 15th WCNDT, Roma 2000

[8] R. Geppert, Pixelsysteme für die Röntgendiagnostik, Dissertation, Uni Freiburg i. Brsg., 1998

[9] X. Llopard, M. Campbell, R. Dinapoli, D. San Segundo, E. Pernigotti, Medipix2, a 64 k Pixel readout chip with 55 μm square elements working in single photon counting mode, Proc. of the IEEE Nuclear Science Symposium and Medical Imaging Conference, San Diego, California, November 4-10, 2001, M7-4, accepted for publication in IEEE Trans.Nucl.Sci.

[10] G. C. Sun et al., Performances of epitaxial GaAs p/i/n structures for X-ray imaging, Nucl. Instr. and Meth. A 487 (2002) 102-106

[11] C. Hordequin, A. Brambilla, P. Bergonzo, F. Foulon, Nuclear radiation detectors using thick amorphous-silicon MIS devices, Nucl. Instr. and Meth. A 456 (2001) 284-289

[12] B. Shulgin, Fast inorganic scintillators, Proceedings of LUMDETR'91, Riga, Latvia, 1991, p.A3

[13] B.C. Grabmaier, New scintillators for X-ray detectors in computed tomography, ibid, p. D6

[14] A. Alybakov, M. Kidibaev, B. Shulgin et all, Inorganic scintillator (on the base of LiF-$UO_2(No_3)_2$, Avt.svidetelstvo SU, N1304584, 19.07.85.

[15] M. Kidibaev, A. Alybakov, L. Victorov, A. Kruzhalov, B. Shulgin, Inorganic scintillator (on the base of LiF-$UO_2(No_3)_2$-CuF_2) Avt.svidetelstvo SU, N1382206, 11.05.1986

[16] M. Kidibaev, A. Alybakov, B. Kenzhebaev, B. Shulgin et all, Thermoluminophor (on the base of LiF-U,Ti. Avt.svidetelstvo SU, N1570509. 0612.1988

[17] B. Shulgin, S. Gorkunova, V. Petrov, D. Shulgin, G. Pilipenko, V. Osipov, Some scintillation properties of HgI_2 single crystals, Proceedings of the International Conference on Inorganic Scintillators and their Applications. Delft, The Netherlands, 1995, p.459-461

[18] G.A. Mesyats, V.I. Solomonov, V.V. Osipov, S.G. Mikhaylov, B.V. Shulgin, V.L.Petrov, Scintillation materials for high current pulse e-beam registration (visualization), ibid, pp.469-471

[19] B. Shulgin, V. Solomonov, S. Mikhailov et all, Inorganic scintillator, Patent RU N2094823, 23. Feb. 1995

[20] V. Solomonov, B. Shulgin, V. Osipov et all, The particular features of pulse cathodoluminescent of HgI_2 , Pisma v Jornal Technical Physics, 1995, v.21, N10, p.29-33

[21] V. Pustovarov, B. Shulgin, E. Zinin et all, Parameters of fast luminescence of Be-P-glasses, Pisma v Jornal Technical Physics, 1996, v.22, p.19-22

[22] L. Zhukova, V. Zhukov, B. Shulgin, Yu. Makurin, Scintillation waveguide, Patent RU, N2154290, 11. May 1999

[23] B. Shulgin, T. Koroleva, V. Petrov, D. Raikov, L. Zhukova, V. Zhukov, Scintillation detector, Patent RU (for Application N2000128437 13. November 2000.)

[24] T.S. Koroleva, M.M. Kidibaev, A.A. Zhamangulov, M.K. Satybaldieva, S.A. Zhaparova, B.V. Shulgin, F.G. Neshov, V.Yu. Yakovlev, Scintillation, absorption and storage properties of (Li,Na)F-U,Me single crystals, First Int. Congress of Radiation Physics, High Current Electronics and Modification of Materials, Tomsk, Russia, 2000, p.436-439

[25] M.M. Kidibaev, T.S. Koroleva, S.A. Zhaparova, M.K. Satybaldieva, K. Musaev, A.A. Zhamangulov, G. Denisov, V. Pustovarov, D. Raikov, B.V. Shulgin, Effect of defect-intrinsic and impurity luminescence for scintillation crystals on the base of (Li,Na)F-U,Me, Sixth Int. Conf. on Inorganic Scintillators and their use in Scientific and Industrial Applications, Chamonix, France, 2001, SM-P_23

[26] I.Ch. Akopjan, B.V. Novikov et all, Pisma v JETP, 1973, v.l7, N8, Pp.419-421

[27] G. Lutz, R. H. Richter, L. Strüder, Novel Pixel Detectors for X-ray Astronomy and Other Applications, 8th Pisa Meeting on Advanced Detectors, Elba, 2000

[28] E. L. Gingold et al., Development of a Novel High-Resolution direct Conversion X-ray Detector, Proc. of SPIE Vol. 3977 (2000)

[29] R. Irsigler, X-ray Imaging Using a 320 x 240 Hybrid GaAs Pixel Detector, IEEE Trans. on Nucl. Science 46 (1999) 507-512

[30] P. G. Pelfer et al., Present status and perspectives of the radiation detectors based on InP materials, Nucl. Instr. and Meth. A 458 (2001) 400-405

[31] G. Zentai et al., Large area Mercuric Iodide X-Ray Imager, Proc. of the SPIE 4682, Medical Imaging, 592 (2002)

[32] R. Göppert, Galliumarsenid CCD-Röntgensensoren, PhD-Thesis, University of Freiburg i. Brsg., 1999

[33] http://www.uni-siegen.de/~ihe/forschung/tfa-technologie.htm

[34] J. Banhart, H. Stanzick, L. Helfen, and T. Baumbach, Metal foam evolution studied by synchrotron radioscopy, Appl. Phys. Lett. **78**, 1152-1154 (2001)

[35] H. Stanzick, M. Wichmann, J. Weise, L. Helfen, T. Baumbach, J. Banhart, Process Control in Aluminum Foam Production Using Real Time X-Ray Radioscopy, Advanced Engineering Materials 4 (2002) 814-823

[36] D. Lübbert, T. Baumbach, J. Härtwig, E. Boller, and E. Pernot, μm-resolved high resolution X-ray diffraction imaging for semiconductor quality control, Nucl. Instr. Meth. B **160** 521-527 (2000)

[37] J. Banhart, H. Stanzick, L. Helfen, T. Baumbach, K. Nijhof, Real-time x-ray investigation of aluminium foam sandwich production, Adv. Eng. Mater., 3 , 2001, 407